

# Distributed formation control with obstacle and collision avoidance for humanoid robot

Faisal Wahab<sup>1</sup>, Bambang Riyanto Trilaksnono<sup>2</sup>

<sup>1</sup>Department of Electrical Engineering, Faculty of Engineering Technology, Parahyangan Catholic University, Bandung, Indonesia

<sup>2</sup>School of Electrical Engineering and Informatics, Bandung Institute of Technology, Bandung, Indonesia

## Article Info

### Article history:

Received Mar 27, 2024

Revised Apr 23, 2025

Accepted Jul 3, 2025

### Keywords:

Collision avoidance

Formation control

Humanoid robot

Multirobot

Obstacle avoidance

## ABSTRACT

Formation control has become a popular research topic in recent years. A common challenge in formation control is ensuring that robots can avoid obstacles and maintain a safe distance from one another to prevent collisions while forming a formation. In this research, a distributed formation control approach for a multi-robot system (MRS) with obstacle and collision avoidance is presented. The distributed formation control architecture is based on a consensus algorithm and consists of four layers: consensus tracking, consensus-based formation control, behavior, and physical robot layers. The system was implemented and evaluated through both simulations and experiments. Humanoid robots were used as the platform for these implementations. The result of the simulations and experiments show that the distributed formation control system successfully guided the robots into desired formation while also avoiding obstacles and preventing collisions with other robots.

*This is an open access article under the [CC BY-SA](https://creativecommons.org/licenses/by-sa/4.0/) license.*



## Corresponding Author:

Faisal Wahab

Department of Electrical Engineering, Faculty of Engineering Technology

Parahyangan Catholic University

Jalan Ciumbuleuit No 94, Bandung, Indonesia

Email: faisal.wahab@unpar.ac.id

## 1. INTRODUCTION

Research and development of robots have increased. In specific applications, a robot not only works independently but also can work simultaneously with others. Robots can cooperate to complete a mission, such as exploration [1] drilling [2]. This type of the robots is called a multi-robot system (MRS). An MRS can effectively complete missions and achieve high-quality performance [3], [4]. One of the most challenging problems in MRS is formation control, where an algorithm is applied to the robots to preserve a desired formation [5].

Recently, formation control has received increasing attention because of its broad application in various fields. Formation control refers to the coordination of multiple agents (such as robots, drones, or autonomous vehicles) to achieve and maintain a specific geometric configuration or formation while moving or operating together. This concept is essential in various applications, including robotics, autonomous systems, and military operations, where a group of agents needs to work collaboratively to achieve a common goal. To accomplish this, control methods and approaches are needed to form and maintain the formation. There are several approaches used for formation control, namely behavior-based [6], leader-follower [7], virtual structure [8], artificial potential field [9], [10], graph-theory based [11], and others. One of these formation control methods is the consensus algorithm [12]. This algorithm incorporates several behaviors, including leader-follower, virtual structure and behavior-based approaches. The basic idea of this algorithm

is that each robot has the ability to update its own information state based on the information state of its nearby neighbors. This process is designed to ensure that every robot ultimately achieves a specific predetermined formation position. The consensus algorithm directs each robot's state towards agreement on a certain value [13].

In the study of formation control, several issues may arise. First, obstacles that must be avoided when forming a formation [14]. Second, there is a possibility of collision among robots as they form the desired formation [15]. These two conditions need to be addressed to ensure that the robots can create the desired formation effectively. In the consensus algorithm, a method for avoiding obstacles and collisions needs to be integrated. Therefore, it is necessary to develop a formation control system based on the consensus algorithm that is capable of avoiding both obstacles and collisions. Many techniques have been proposed by researchers to address obstacle and collision avoidance. The potential field method [16] is one solution for obstacle avoidance, but it has a weakness, when obstacles are located at desired position, the target may become inaccessible. The fuzzy neural network method [17] requires separate control from formation control, which can place a burden on humanoid robot's computing resources. The final method is Stipanovic's method [18], which addresses the collision avoidance problem through the Lyapunov analysis method. Since this method is based on a central point with layer of communication radius, it can be used for both obstacle and collision avoidance. For a differentially-driven mobile robot, this approach can merge the two key control challenges, trajectory tracking and obstacle-collision avoidance, into one unified motion control algorithm. Because the motion control layer addresses the collision avoidance issue, the trajectory does not need to be replanned [19].

The primary goal of this paper is to design and implement formation control with obstacle and collision avoidance through simulation and experiment. The formation control approach presented is distributed consensus algorithm enhanced with an obstacle and collision avoidance method. To verify that this design function properly, simulations and experiments are conducted. Generally, formation control is implemented using mobile robots. In this paper, a humanoid robot is used in both simulations and experiments. The type of humanoid robot used is the NAO humanoid Aldebaran robot [20]. This robot has features that are quite capable of being used for formation control but has limitations in internal odometry [21]. Achieving precise odometry with a humanoid robot is challenging due to its large number of degrees of freedom, inaccurate actuators, and slipping feet. Therefore, an external camera is required to identify the position and orientation of each robot throughout the navigation process [22]. By using the camera as feedback, the humanoid robot can walk according to the desired position. The result of the simulation and experiment will be shown in two dimensions.

## 2. METHOD

In this section, the architecture of a consensus-based distributed formation control system with the ability to avoid obstacles and collisions is presented. The adopted architecture follows a layered approach [12]. The design consists of four layers: consensus tracking, consensus-based control, behavior, and physical robot layers. In Figure 1,  $\mathcal{N}_i(t)$  denotes the group of vehicles whose coordination variable representations are available to robots  $i$  at time  $t$ , and  $J_i(t)$  denotes the position of tracking errors.  $\xi_j = [x_{cj}, y_{cj}, \theta_{cj}]^T$  represents the coordination variable of the robots object. In this paper, value  $\xi_j$  cannot be obtained directly from neighboring robots due to low precision of the robots' odometry [21]. Therefore, it is replaced with a visual-based localization system using a camera. The designed architecture follows the consensus algorithm framework. An explanation of each layer will be discussed in the next subsection.

### 2.1. Consensus tracking layer

The first layer is consensus tracking, whose objective is to drive  $\xi_i$  toward  $\xi^r$ . Here  $\xi_i = [x_{ci}, y_{ci}, \theta_{ci}]^T$  is the robot's actual position and orientation of the  $i$ -th robot, while  $\xi^r = [x_c^r, y_c^r, \theta_c^r]^T$  denotes the reference coordination variable, also known as consensus reference state. In this scenario, the reference corresponds to the desired state defined by the virtual structure approach. The fundamental concept involves assigning a virtual leader, or employing virtual structure approach, positioned at the virtual center of the formation, to serve as a reference point for the entire group. This allows the desired states of each vehicle to be specified in relation to the virtual structure approach. To determine the exchange of information between the virtual structure and each robot in a formation, graph theory is used.

A model for information exchange among robots in formation control can be based on either directed or undirected graph theory. A directed tree is a type of structure where each node has one parent, except for one special node called the root, which has no parent. In the consensus reference state framework, the reference state  $\xi^r$  and its derivative  $\dot{\xi}^r$  are accessible only to a subgroup of the followers, referred to as subgroup leaders. These subgroup leaders are the vehicles that have direct access to reference information.

Consensus tracking with a consensus reference state is achieved if  $\xi_i \rightarrow \xi^r$  as  $t \rightarrow \infty$  for all  $i = 1, \dots, n$ , and this holds if and only if the interaction topology includes a directed spanning tree. A directed spanning tree is a directed tree that connects all of the nodes in graph, ensuring information flow from the root to every other node. Within the consensus tracking layer, each the robot implements a consensus tracking algorithm as defined in (1).

$$u_i = \frac{1}{\eta_i(t)} \sum_{j=1}^n a_{ij}^c(t) [\xi_j - \gamma(\xi_i - \xi_j)] + \frac{1}{\eta_i(t)} a_{i(n+1)}^c(t) [\xi^r - \gamma(\xi_i - \xi^r)], \quad i = 1, \dots, n \quad (1)$$

Here,  $\eta_i(t) \triangleq \sum_{j=1}^{n+1} a_{ij}^c(t)$ , where  $a_{ij}^c$  for  $i = 1, \dots, n$ , and  $j = 1, \dots, n+1$ , represent the  $(i, j)$ -th entry of adjacency matrix  $A_{n+1}^c \in \mathbb{R}^{(n+1) \times (n+1)}$  at time  $t$ ,  $\gamma$  is a positive scalar.

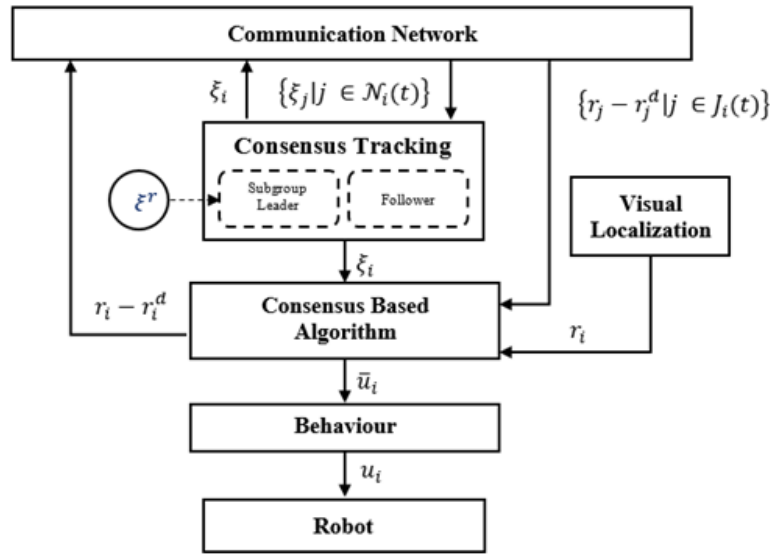


Figure 1. Distributed formation control architecture

## 2.2. Consensus based formation control

Assuming the robots' dynamics follow a single-integrator model,  $\dot{r}_i = u_i$  for  $i = 1, \dots, n$ , where  $\dot{r}_i \in \mathbb{R}^m$  represents the state and  $u_i \in \mathbb{R}^m$  is the control input of the  $i$ -th robot. Consensus is achieved if the states converge to a constant value equal to the weighted average of the initial state information of all robots. At the robot control level, a consensus algorithm is implemented in (2).

$$u_i = \dot{r}_i^d - \alpha_i(r_i - r_i^d) - \sum_{j=1}^n a_{ij}^v[(r_i - r_i^d) - (r_j - r_j^d)] \quad (2)$$

Where  $\alpha_i$  is a positive scalar, and  $a_{ij}^v$  is the  $(i, j)$ -th entry of the  $n \times n$  adjacency matrix  $A_n^v$  associated with the interaction topology  $G_n^v \triangleq (V_n^v, E_n^v)$  for  $(r_i - r_i^d)$ . Here,  $r_i = [x_i, y_i]^T$  is the actual position of the  $i$ -th robot,  $r_i^d = [x_i^d, y_i^d]^T$  is the desired position, and  $r_{iF}^d = [x_{iF}^d, y_{iF}^d]^T$  is the intended deviation of the  $i$ -th robot relative to  $C_F$ , which represents a virtual coordinate frame positioned at a virtual center  $(x_c, y_c)$ . The objective is to track  $C_o$  as the inertial frame relative to  $C_F$  within the virtual leader/virtual structure, as defined in (3).

$$\begin{bmatrix} x_i^d \\ y_i^d \end{bmatrix} = \begin{bmatrix} x_{ci} \\ y_{ci} \end{bmatrix} + \begin{bmatrix} \cos[\theta_{ci}] & -\sin[\theta_{ci}] \\ \sin[\theta_{ci}] & \cos[\theta_{ci}] \end{bmatrix} \begin{bmatrix} x_{iF}^d \\ y_{iF}^d \end{bmatrix} \quad (3)$$

When  $\xi_i \rightarrow \xi^r$  and  $r_i \rightarrow r_i^d$ , for  $i = 1, \dots, n$ , as  $t \rightarrow \infty$ , the desired formation is preserved, and the state of the virtual coordinate frame tracks the desired reference.

### 2.3. Behavior layer

The behavior layer is composed of two components: obstacle avoidance and collision avoidance. The obstacle avoidance function enables each robot to detect and navigate around obstacles along its path, while collision avoidance ensures that robots maintain safe distances from one another during formation to prevent inter-robot collisions.

Figure 2 shows the obstacle and collision avoidance areas [23]. Where  $\Psi_i = \{x \in \mathbb{R}^2 | \|r_i - r_j\|_2 \leq r_c\}$  is a collision region,  $\Phi_i = \{x \in \mathbb{R}^2 | r_c \leq \|r_i - r_j\|_2 \leq r_b\}$  is a collision avoidance region, and  $\Omega_i = \{x \in \mathbb{R}^2 | r_c \leq \|r_i - r_j\|_2 \leq r_a\}$  is the communication region.

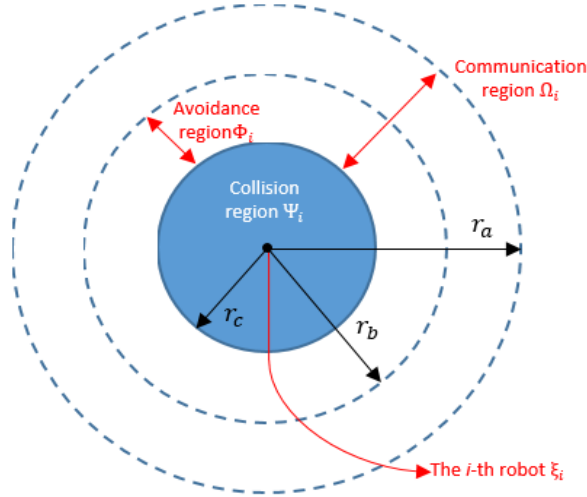


Figure 2. Sectional drawing of the defined regions for the  $i$ -th robots

The obstacle avoidance is given by (4).

$$\frac{\partial V_{iobs}}{\partial r_i} = \begin{cases} \frac{4(r_c^2 - r_b^2)(r_b^2 - \|r_i - r_j\|_2^2)}{(\|r_i - r_j\|_2^2 - r_c^2)^2} (r_i - r_j)^T & r_c \leq \|r_i - r_j\|_2 \leq r_b \\ 0 & \|r_i - r_j\|_2 \geq r_b \end{cases} \quad (4)$$

The collision avoidance is given by (5).

$$\frac{\partial V_{ij}}{\partial r_i} = \begin{cases} \frac{4(r_c^2 - r_b^2)(r_b^2 - \|r_i - r_j\|_2^2)}{(\|r_i - r_j\|_2^2 - r_c^2)^2} (r_i - r_j)^T & r_c \leq \|r_i - r_j\|_2 \leq r_b \\ 0 & \|r_i - r_j\|_2 \geq r_b \end{cases} \quad (5)$$

At the level of the robot physically, the consensus-based formation control layer is combined with the obstacle avoidance method (4) and collision avoidance method (5). Control of each robot becomes, as in (6).

$$u_i = \dot{r}_i^d - \alpha_i(r_i - r_i^d) - \sum_{j=1}^n a_{ij}^v [(r_i - r_i^d) - (r_j - r_j^d)] - \sum_{obs=1}^m \frac{\partial V_{iobs}}{\partial r_i} - \sum_{j=1}^n \frac{\partial V_{ij}}{\partial r_i} \quad (6)$$

In (6), the term  $\dot{r}_i^d - \alpha_i(r_i - r_i^d) - \sum_{j=1}^n a_{ij}^v [(r_i - r_i^d) - (r_j - r_j^d)]$  is used to maintain consensus, while the terms  $-\sum_{obs=1}^m \frac{\partial V_{iobs}}{\partial r_i}$  is used to avoid obstacle, and the term  $-\sum_{j=1}^n \frac{\partial V_{ij}}{\partial r_i}$  is used to avoid collisions among robot.

### 2.4. Physically robot layer

The humanoid robots used in this study are NAO robots developed by Aldebaran. Each NAO robot stands 58 cm tall, weighs approximately 4.3 kg, and has 25 degrees of freedom, enabling for a wide range of movements. The robot is equipped with an integrated multimedia system that includes four microphones, two

speakers, and two cameras. In addition, it contains a 2-axis gyroscope, a 3-axis accelerometer, and several force-sensitive resistors. NAO comes with its own control software, which includes graphical programming through “Choregraphe,” simulation capabilities via Naosim, and a development kit (Naoqi SDK). It runs on a Linux-based operating system and supports programming in multiple languages such as C++, Python, Java, Urbi, and MATLAB. For communication, NAO is equipped with Ethernet, Wi-Fi, and infrared connectivity options.

### 3. RESULTS AND DISCUSSION

This section presents both simulation and experimental results. The simulations are conducted to evaluate the performance of the proposed control system and verify its ability to achieve the desired formation. Both the simulation and the physical experiment involve four humanoid robots, each moving according to its actual step length. In both cases, the robots and obstacles are positioned identically to ensure consistency between the simulated and real-world environments.

Before conducting the simulation and experiment, it is necessary to determine the topology between the robots. This interaction topology is used to exchange information through the consensus algorithm for all robots. The interaction topology designed in this study is shown in Figure 3. The designed topology consists of a leader and followers, where the leader is a virtual structure in the consensus algorithm and the followers are the humanoid robots [24].

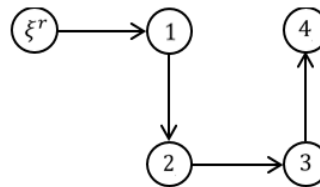


Figure 3. Interaction topology

#### 3.1. Simulation results

The number of humanoid robots used in the simulation is four, with each humanoid robot represented by a dot of a different color. The formation used in the simulation is a marching formation, and three obstacles are placed randomly for the robot to avoid. Each obstacle is defined by a minimum and maximum safe distance: 0.45 meters and 0.5 meters, respectively. Several conditions are analyzed, including the simulation of robot positions in two dimensions, a graph of the distance among robots, and a graph of the error for each robot relative to the desired position. The starting position of the robots are assigned randomly, but arranged so that they remain sequentially close to each other.

As shown in Figure 4, the marching formation was successfully established. As the robots navigate, those approaching obstacles are able to avoid them. When a robot enters an obstacle’s safety layer, it deviates from the desired trajectory. These deviations may disrupt the trajectories of nearby robots. If a robot encounters another robot deviating to avoid an obstacle, it adjusts its motion to maintain a safe distance.

Figure 5 shows the distance of each robot, demonstrating that the robots are able to maintain the desired formation while avoiding obstacles and collisions. The graph analyzes the likelihood of collisions based on the distances between robots. In the marching formation, robot 1 is positioned at the bottom of the graph and robot 4 at the top, with a desired uniform spacing of 0.75 meters. By observing the distance variations as the robots avoid obstacles, it can be seen that the trajectory of robot 3 intersects with an obstacle’s communication radius. When robot 3 avoids the obstacle, it deviates from its path and approaches robot 4. This triggers the collision avoidance method, which successfully prevents a collision between 60-70 seconds. In the second condition, during the 90-100 second interval, robots 2 and 3 maintain their distances effectively, ensuring no collisions occur.

In Figure 6, the graph shows the error in each robot’s actual position relative to the desired position on the  $x$  and  $y$  axis. The error approaches zero when the desired position matches the actual position ( $|x_r - x_i| \rightarrow 0$ ,  $|y_r - y_i| \rightarrow 0$ ). With 10 seconds, all robots reach their desired positions. Between 50 and 110 seconds, the error fluctuates as the robots deviate from their trajectories to avoid obstacles and collisions.

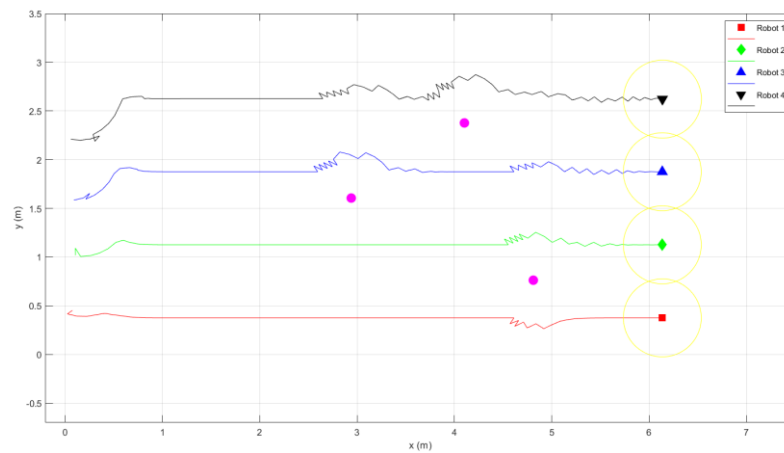


Figure 4. Simulation results of a marching formations

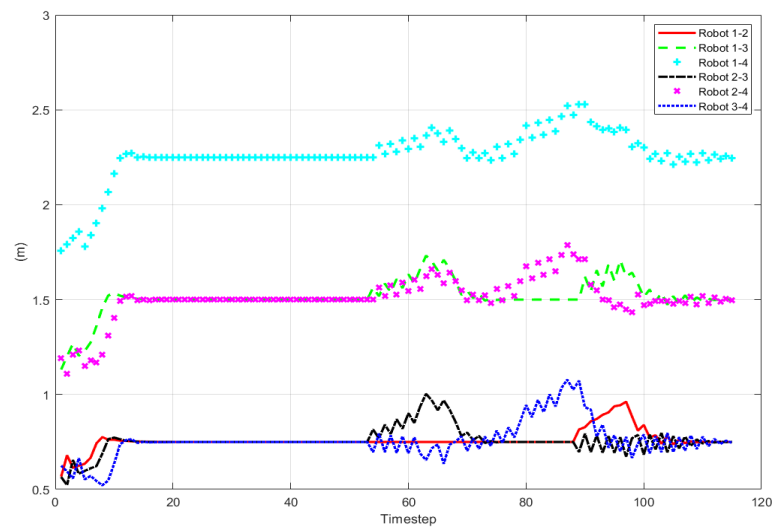


Figure 5. Graph of the distance among robots

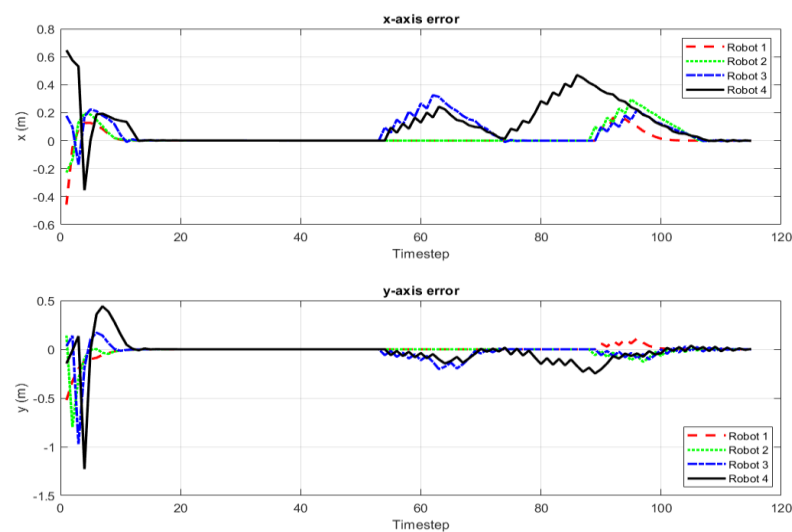


Figure 6. Graph of X and Y axis error for each robot relative to the desired position in simulation

### 3.2. Experimental results

The experimental setup for formation control consists of four Aldebaran NAO humanoid robot, a PC/laptop, a router, and a webcam camera. The experiment is conducted in an indoor area measuring  $3 \times 7$  meters. A camera is positioned 3.5 meters above the floor to detect the position and orientation of each robot using image processing on a laptop. Each robot is equipped with a different colored marker placed on top of the humanoid robot's head. The marker is shaped like a pentagon, with the front extended and sharpened to determine the robot's orientation angle. The obstacles are round and distinguished by different colors. The experiment follows the same pattern as the simulation, namely a marching formation with three obstacles.

As shown in Figure 7, the marching formation was successfully established. However, the humanoid robots were unable to walk in a perfectly straight line due to distortion issues in image processing, which require further investigation [25]. Despite this issue, the robots were still able to maintain the desired formation trajectory. This demonstrates the effectiveness of the formation control strategy, including obstacle and collision avoidance, in guiding the robots to maintain formation while reaching the desired positions.

Based on the inter-robot distance graph shown in Figure 8, each robot was able to maintain a minimum separation radius of 0.45 meters from the others. The smallest distance was observed between Robot 3 and Robot 4 during obstacle avoidance. Nevertheless, a collision was successfully prevented when the collision avoidance algorithm was activated for Robot 4. To demonstrate consensus, Figure 9 presents the position errors in both the x and y axes for each robot relative to their desired positions, which coincide with their actual final positions ( $|x_r - x_i| \rightarrow 0$ ,  $|y_r - y_i| \rightarrow 0$ ).

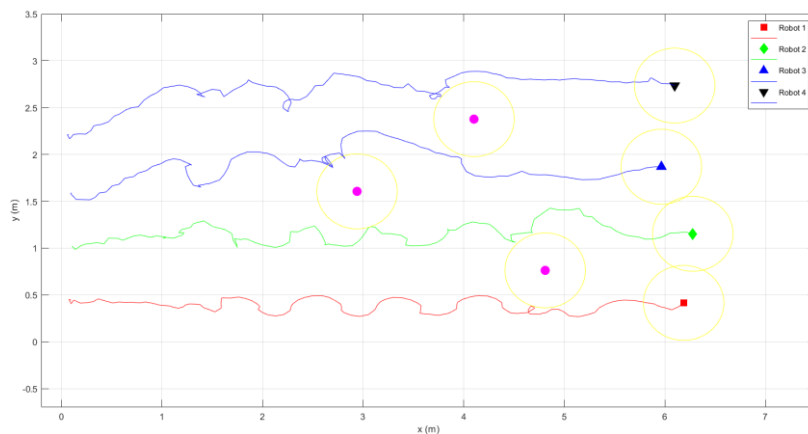


Figure 7. Experimental results of the marching formations

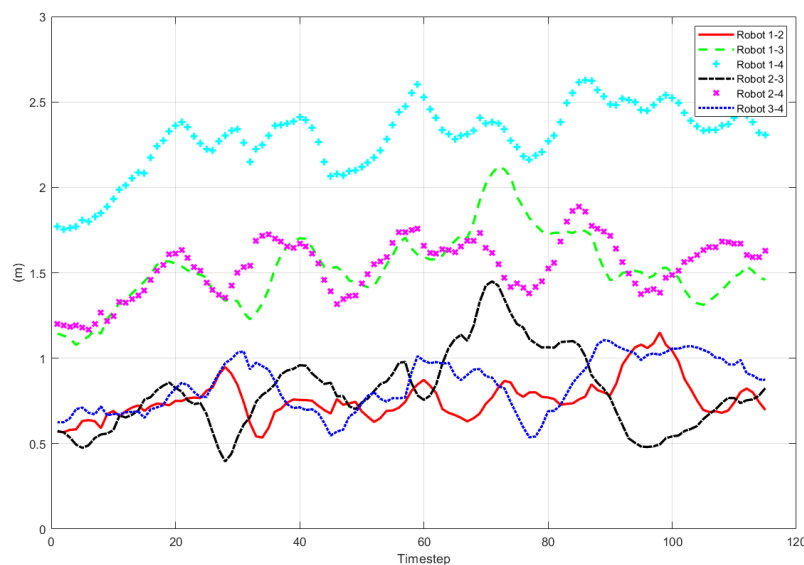


Figure 8. Graph of inter-robot distances

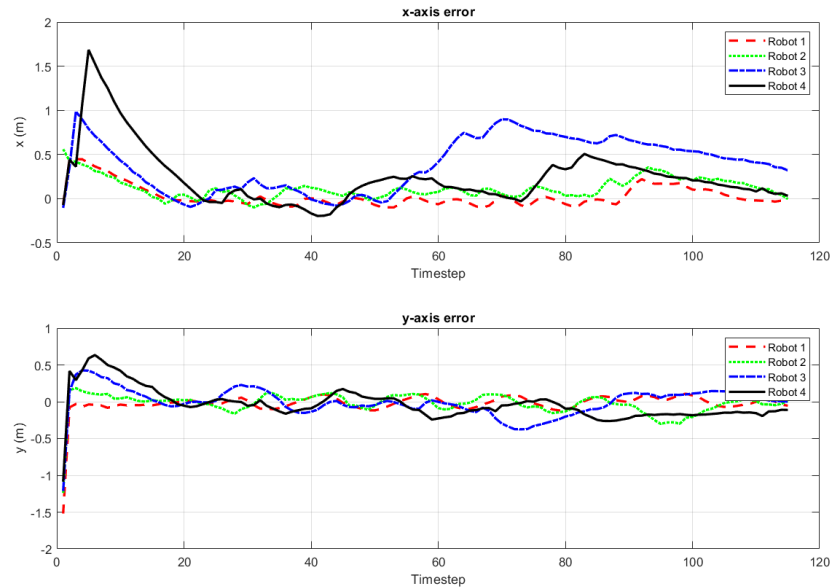


Figure 9. Graph of position errors along the x- and y-axes for each robot relative to the desired position in the experiment

This section discusses the differences between the simulation and experimental results. In the simulation, the robots achieved the formation faster and with more stable movement compared to the experiment. The main issue in this experiment were camera distortion and a slippery surface. Camera distortion caused discrepancies between the actual positions and those shown on camera screen, while slippery surfaces made it difficult for the robots to move in a straight line. However, the consensus algorithm kept the robots in the desired formation. In another experiment, an obstacle was placed farther away than before. As a result, the robots had to deviate from their trajectory, making it difficult to maintain the formation. The formation could not be achieved due to the limited number of iterations and the restricted area covered by the camera.

Figure 10 shows a snapshot from the experiment in the indoor area. A pentagon-shape marker with different colors was attached to the top of each humanoid robot's head. Each marker had a different color for both the humanoid robots and the obstacles. This differentiation simplified image processing and programming. The floor in image appears asymmetrical due to distortion issues in image processing. This distortion causes discrepancies between the position and distance on the screen compared to the actual conditions.

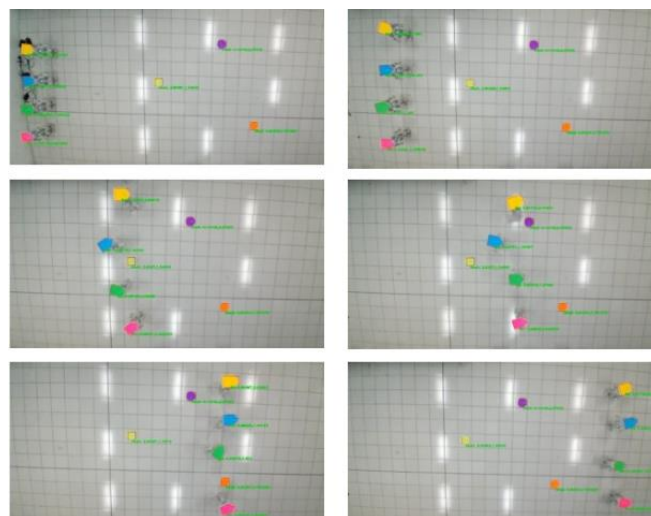


Figure 10. Snapshot of the experimental setup for formation control



#### 4. CONCLUSION

In this paper, the main objective is to design a distributed formation control system for humanoid robots that incorporates obstacle and collision avoidance capabilities using visual localization. Based on the results of simulations and experiments, the distributed formation control system was successfully applied to a group of humanoid robots, enabling them to form the desired formation while avoiding obstacles and collisions. Both the simulation and the experiment achieved consensus and established a marching formation. Throughout each step, the robots in both the simulation and experiment adhered to the humanoid robot's step specifications. However, several differences were observed: The number of iterations in the simulation and experiment differed due to image processing distortions from the camera. These distortions affected robot movement because of discrepancies between the information captured by the camera and the actual environment. When an obstacle had a large communication range and was placed too far away, the robot deviated from their paths, preventing them from reaching the desired positions. For future work, development efforts should focus on reducing distortion in image processing to improve the accuracy of camera's view relative to the real environment. In addition, other robot platforms, such as differential mobile robots, should be explored for smoother movement. Further studies will be conducted to design various topologies for virtual trajectories, ensuring the formation can follow them effectively.

#### FUNDING INFORMATION

Authors state no funding involved.

#### AUTHOR CONTRIBUTIONS STATEMENT

This journal uses the Contributor Roles Taxonomy (CRediT) to recognize individual author contributions, reduce authorship disputes, and facilitate collaboration.

Name of Author	C	M	So	Va	Fo	I	R	D	O	E	Vi	Su	P	Fu
Faisal Wahab		✓	✓	✓	✓	✓	✓	✓	✓	✓	✓			
Bambang Riyanto	✓	✓			✓	✓	✓	✓	✓			✓		
Trilaksono														

C : Conceptualization

M : Methodology

So : Software

Va : Validation

Fo : Formal analysis

I : Investigation

R : Resources

D : Data Curation

O : Writing - Original Draft

E : Writing - Review & Editing

Vi : Visualization

Su : Supervision

P : Project administration

Fu : Funding acquisition

#### CONFLICT OF INTEREST STATEMENT

Authors state no conflict of interest.

#### DATA AVAILABILITY

Derived data supporting the findings of this study are available from the corresponding author Faisal Wahab on request.




#### REFERENCES

- [1] A.-C. Stan, "A decentralised control method for unknown environment exploration using Turtlebot 3 multi-robot system," in *2022 14th International Conference on Electronics, Computers and Artificial Intelligence (ECAI)*, 2022, pp. 1–6, doi: 10.1109/ECAI54874.2022.9847497.
- [2] D. D. K. Nguyen, Y. Lai, S. Sutjipto, and G. Paul, "Hybrid multi-robot system for drilling and blasting automation," in *2020 16th International Conference on Control, Automation, Robotics and Vision (ICARCV)*, 2020, pp. 79–84, doi: 10.1109/ICARCV50220.2020.9305391.
- [3] B. Xu, "Institute of Electrical and Electronics Engineers. Beijing Section, and Institute of Electrical and Electronics Engineers," *Proceedings of 2019 IEEE 8th Joint International Information Technology and Artificial Intelligence Conference (ITAIC 2019): May 24-26, 2019, Chongqing, China*.
- [4] V. Ababii, V. Sudacevschi, R. Braniste, A. Nistiriuc, S. Munteanu, and O. Borozan, "Multi-robot system based on swarm intelligence for optimal solution search," in *2020 International Congress on Human-Computer Interaction, Optimization and Robotic Applications (HORA)*, 2020, pp. 1–5, doi: 10.1109/HORA49412.2020.9152926.
- [5] C. Wang, H. Tnunay, Z. Zuo, B. Lennox, and Z. Ding, "Fixed-time formation control of multirobot systems: design and experiments," *IEEE Transactions on Industrial Electronics*, vol. 66, no. 8, pp. 6292–6301, Aug. 2019, doi: 10.1109/TIE.2018.2870409.




- [6] S. Li *et al.*, “Experimental research on formation control of UAVs based on behavior rules,” in *2022 41st Chinese Control Conference (CCC)*, 2022, pp. 4495–4500, doi: 10.23919/CCC55666.2022.9901535.
- [7] A. Alfaro and A. Moran, “Leader-follower formation control of nonholonomic mobile robots,” in *2020 IEEE ANDESCON, ANDESCON 2020, Institute of Electrical and Electronics Engineers Inc.*, Oct. 2020, doi: 10.1109/ANDESCON50619.2020.9272048.
- [8] H. Wang, Y. Huang, J. Chu, and S. Sun, “A virtual structure approach to formation control of multi robots with collision avoidance in space station,” in *2022 41st Chinese Control Conference (CCC)*, 2022, pp. 4897–4902, doi: 10.23919/CCC55666.2022.9902358.
- [9] Y. Yan, J. Li, H. Dong, C. Gao, and Y. Fang, “An improved artificial potential field method for formation control and obstacle avoidance of the multi-agents systems,” in *2023 China Automation Congress (CAC)*, 2023, pp. 2877–2882, doi: 10.1109/CAC59555.2023.10451358.
- [10] Y. Zhao, L. Jiao, R. Zhou, and J. Zhang, “UAV formation control with obstacle avoidance using improved artificial potential fields,” in *2017 36th Chinese Control Conference (CCC)*, 2017.
- [11] H. T. T. Nguyen, H. T. Do, H. T. Tran, and M. T. Nguyen, “Collision-free distributed formation control of multi-agent systems based on formation graph,” in *2023 International Conference on Control, Robotics and Informatics (ICCRI)*, 2023, pp. 34–38, doi: 10.1109/ICCRI58865.2023.00014.
- [12] W. Ren and R. W. Beard, *Distributed Consensus in Multi-vehicle Cooperative Control*, in *Communications and Control Engineering*, London: Springer London, 2008, doi: 10.1007/978-1-84800-015-5.
- [13] W. Ren and N. Sorensen, “Distributed coordination architecture for multi-robot formation control,” *Robotics and Autonomous Systems*, vol. 56, no. 4, pp. 324–333, 2008, doi: 10.1016/j.robot.2007.08.005.
- [14] L. He, R. Xiao, B. Gao and W. Huang, “Distributed finite time formation control and obstacle avoidance for UAV swarms,” *2024 36th Chinese Control and Decision Conference (CCDC)*, Xi'an, China, 2024, pp. 3031–3036, doi: 10.1109/CCDC62350.2024.10587391.
- [15] J. Zhou, Y. Guo, G. Li, and J. Zhang, “Event-triggered control for nonlinear uncertain second-order multi-agent formation with collision avoidance,” *IEEE Access*, vol. 7, pp. 104489–104499, 2019, doi: 10.1109/ACCESS.2019.2929540.
- [16] S. M. H. Rostami, A. Kumar, J. Wang, and X. Liu, “Obstacle avoidance of mobile robots using modified artificial potential field algorithm,” *EURASIP Journal on Wireless Communications and Networking*, vol. 2019, 2019, doi: 10.1186/s13638-019-1396-2.
- [17] L. Guan, Y. Lu, Z. He, and X. Chen, “Intelligent obstacle avoidance algorithm for mobile robots in uncertain environment,” *Journal of Robotics*, vol. 2022, 2022, doi: 10.1155/2022/8954060.
- [18] P. F. Hokayem, D. M. Stipanović, and M. W. Spong, “Coordination and collision avoidance for Lagrangian systems with disturbances,” *Applied Mathematics and Computation*, vol. 217, no. 3, pp. 1085–1094, Oct. 2010, doi: 10.1016/j.amc.2010.03.074.
- [19] W. Kowalczyk, M. Michałek, and K. Kozłowski, “Trajectory tracking control and obstacle avoidance for a differentially driven mobile robot,” *IFAC Proceedings Volumes*, vol. 44, no. 1, pp. 1058–1063, 2011, doi: 10.3182/20110828-6-IT-1002.03567.
- [20] G. Oriolo, A. Paolillo, S. Michieletto, and E. Menegatti, “Human action recognition oriented to humanoid robots action reproduction,” in *Proceedings of the AI\*IA Workshop and Prize*, Italy, Jun. 2012, pp. 35–40.
- [21] G. Oriolo, A. Paolillo, R. Lorenzo, and M. Venditelli, “Vision-based odometric localization for humanoids using a kinematic EKF,” in *12th International Conference on Humanoid Robots*, Japan, Nov. 2012, pp. 153–158.
- [22] G. Oriolo, A. Paolillo, L. Rosa, and M. Venditelli, *Vision-Based Trajectory Control for Humanoid Navigation*. IEEE, 2013.
- [23] Z. Sun and Y. Xia, “Consensus-based formation control with dynamic role assignment,” *Chinese: 26th Chinese Control and Decision Conference*, 2014, pp. 3681–3686.
- [24] D. Sabir and Q. Wu, “Cooperative tracking control and obstacles avoidance for single-integrator dynamics,” in *Proceedings of the 32nd Chinese Control Conference*, China, Jul. 2013, pp. 7162–7167.
- [25] C. Paredes-Orta, L. M. Valentin-Coronado, A. Díaz-Ponce, J. Rodríguez-Reséndiz, and J. D. Mendiola-Santibañez, “Distortion calculation method based on image processing for automobile lateral mirrors,” *Micromachines (Basel)*, vol. 13, no. 3, 2022, doi: 10.3390/mi13030401.

## BIOGRAPHIES OF AUTHORS



**Faisal Wahab**    received the B.Eng. degree in electrical engineering education from Indonesia University of Education, Indonesia, in 2011 and the M.S. degrees in School of Electrical Engineering and Informatics at Bandung Institute of Technology in 2015. Currently, he is a lecturer at Parahyangan Catholic University in the Electrical Engineering Program with a concentration in mechatronics. His research interests include robotics, modelling system, electronics, intelligent control system. He can be contacted at email: faisal.wahab@unpar.ac.id.



**Bambang Riyanto Trilaksono**    was graduated from Electrical Engineering Dept., Institut Teknologi Bandung (ITB), Indonesia, in 1986. He obtained his Master and Doctoral Degrees both from Electrical Engineering Dept, Waseda University, Japan, in 1991 and 1994, respectively. He is a professor at School of Electrical Engineering and Informatics, Bandung Institute of Technology. His research interests include optimal control, robust control, embedded control systems AI and robotics. He can be contacted at email: briyanto@lskk.ee.itb.ac.id.